4-9-2003

Cole-Cole Analysis of the Superspin Glass System $Co_{80}Fe_{20}/Al_2O_3$

O. Petracic
Laboratorium für Angewandte Physik, Gerhard-Mercator-Universität Duisburg

Sarbeswar Sahoo
Laboratorium für Angewandte Physik, Gerhard-Mercator-Universität Duisburg, sarbeswar@gmail.com

Christian Binek
University of Nebraska-Lincoln, cbinek@unl.edu

Wolfgang Kleemann
Laboratorium für Angewandte Physik, Gerhard-Mercator-Universität Duisburg, wolfgang.kleemann@uni-due.de

J.B. Sousa
IFIMUP, Departamento de Fisica, Universidade de Porto, 4169-007 Porto, Portugal

See next page for additional authors

Published in *Phase Transitions* 76:4–5 (2003), pp. 367–375. http://www.tandf.co.uk/journals/titles/01411594.asp

Cole-Cole Analysis of the Superspin Glass System $Co_{80}Fe_{20}/Al_2O_3$

O. Petracic[a,*], S. Sahoo[a], Ch. Binek[a], W. Kleemann[a], J. B. Sousa[b], S. Cardoso[c], and P. P. Freitas[c]

[a] Laboratorium für Angewandte Physik, Gerhard-Mercator-Universität Duisburg, 47048 Duisburg, Germany
[b] IFIMUP, Departamento de Fisica, Universidade de Porto, 4169-007 Porto, Portugal
[c] INESC, Rua Alves Redol 9-1, 1000 Lisbon, Portugal

Abstract: Ac susceptibility measurements were performed on discontinuous magnetic multilayers $[Co_{80}Fe_{20}(t)/Al_2O_3(3\ nm)]_{10}$, $t = 0.9$ and 1.0 nm, by Superconducting Quantum Interference Device (SQUID) magnetometry. The CoFe forms nearly spherical ferromagnetic single-domain nanoparticles in the diamagnetic Al_2O_3 matrix. Due to dipolar interactions and random distribution of anisotropy axes the system exhibits a spin-glass phase. We measured the ac susceptibility as a function of temperature $20 \leq T \leq 100$ K at different dc fields and as a function of frequency $0.01 \leq f \leq 1000$ Hz. The spectral data were successfully analyzed by use of the phenomenological Cole–Cole model, giving a power-law temperature dependence of the characteristic relaxation time τ_c and a high value for the polydispersivity exponent, $\alpha \approx 0.8$, typical of spin glass systems.

Keywords: Multilayers, Ac susceptibility, Polydispersivity, Dipolar interactions, Spin-glass behavior

1. INTRODUCTION

The dynamic and static magnetic properties of spin glasses (SG) are still a subject of intense experimental and theoretical research. In the field of experiments a vast variety of different spin glass systems (Young, 1997) have yet been found and investigated. A rather new class are the so-called superspin glass (SSG) systems (Kleemann *et al.*, 2001). Here the sample is composed of an ensemble of dipolarly interacting nanoparticles, each having a superspin moment in the order of 1000 μ_B. The SG properties are due to frustration, a natural property of dipolar interaction, and to randomness of the anisotropy axis directions, frequently also of the spin sizes. Two different types of realizations of SSG systems exist, frozen ferrofluids (Djurberg *et al.*, 1997; Dormann *et al.*, 1997, 1999; Mamiya *et al.*, 1999) and discontinuous magnetic multilayers (Sankar *et al.*, 2000; Kleemann *et al.*, 2001; Sousa *et al.*, 2001; Petracic *et al.*, 2002; Sahoo *et al.*, 2002a).

*Corresponding author. E-mail: petracic@kleemann.uni-duisburg.de

It is widely accepted that 3-dimensional (3D) nanoparticle systems with high enough density of the particles and sufficiently narrow particle size distribution do have SG properties, i.e. there exists a phase transition temperature, T_g, where the characteristic relaxation time and the static nonlinear susceptibility diverge (Djurberg *et al.*, 1997; Kleemann *et al.*, 2001; Petracic *et al.*, 2002; Sahoo *et al.*, 2002a). In order to observe SSG properties the collective glass temperature, T_g, has to be larger than the so-called blocking temperature, T_b, at which the relaxation time of the individual moments (Néel, 1949; Brown, 1963)

$$\tau = \tau_0 \exp(KV/k_BT), \tag{1}$$

reaches the order of the timescale of the experiment. Here K is the effective anisotropy constant of one nanoparticle, V the volume and $\tau_0 \sim 10^{10}$ s the relaxation time at $T \rightarrow \infty$. Below T_b the particle moments are "blocked."

The condition $T_g < T_b$ is met in our discontinuous metal–insulator multilayers (DMIMs) $[Co_{80}Fe_{20}(t)/Al_2O_3(3\text{ nm})]n$, where $t \leq 1{:}0$ nm is the nominal thickness of the ferromagnetic CoFe layers and n the number of bilayers. The CoFe does not form a continuous layer but forms nearly spherical particles embedded in the diamagnetic Al_2O_3 matrix (Kakazei *et al.*, 2001). One finds self-organized arrangements of particles in each layer (Stappert *et al.*, 2002), i.e., the interparticle distances are nearly constant. While SSG behavior is found for relatively small values of $t \leq 1.0$ nm and $n = 10$ (Kleemann *et al.*, 2001; Petracic *et al.*, 2002; Sahoo *et al.*, 2002a), for higher values of the nominal thickness, $1.0 < t \leq 1.4$ nm, superferromagnetism (SFM) is observed (Kleemann *et al.*, 2001; Chen *et al.*, 2002; Sahoo *et al.*, 2002b).

In this article we will focus on the SSG systems $[Co_{80}Fe_{20}(t)/Al_2O_3\ (3\text{ nm})]_{10}$, with $t = 0.9$ and 1.0 nm. The existence of a SG phase was evidenced by means of dynamic criticality, static criticality of the nonlinear susceptibililty and dynamical scaling (Kleemann *et al.*, 2001; Petracic *et al.*, 2002; Sahoo *et al.*, 2002a). All three methods yield convincing values for the glass transition temperature and the dynamical critical exponents, respectively, $T_g \approx 44$K, $z\nu \approx 9.5$, $\gamma \approx 1.47$ and $\beta \approx 1.0$ for $t = 0.9$ nm and $T_g \approx 49$K, $z\nu \approx 10.0$, $\gamma \approx 1.36$ and $\beta \approx 0.6$ for $t = 1.0$ nm. T_g and $z\nu$ are the error weighted average values obtained from different methods.

While $z\nu$ characterizes the divergence of the relaxation time of the largest ordered cluster as $T \rightarrow T_g$, there is a wide distribution of shorter relaxation times due to nonpercolating clusters. They are characteristic of the glassy nature of the system and deserve a focused investigation, which will be described in the present paper. To this end we analyze the results of measurements of the complex ac susceptibility carried out at different ac amplitudes and bias fields and frequencies f. In particular the so-called Cole–Cole presentation, χ'' *vs* χ', will be discussed in terms of appropriate empirical models of relaxational polydispersivity.

2. EXPERIMENTAL

The DMIM samples $Glass/Al_2O_3(3\text{ nm})/[Co_{80}Fe_{20}(t)/Al_2O_3\ (3\text{ nm})]_{10}$ ($t = 0.9$ and 1.0 nm) are prepared by sequential Xe ion beam sputtering from two separate targets

(Kakazei *et al.*, 2001). The CoFe forms nearly spherical granules of approximately 3 nm diameter and 2 nm interparticle spacing as found from transmission electron microscopy (TEM) studies (Stappert *et al.*, 2002).

The measurements were performed by use of a commercial Superconducting Quantum Interference Device (SQUID) magnetometer (MPMS-5S, Quantum Design). The ac susceptibility, $\chi = \chi' - i\chi''$, is extracted from the linear response of the sample on an oscillating ac field, $\mu_0 H_{ac} = 0.05$ or 0.4 mT at different ac frequencies, $0.01 \leq f \leq 1000$ Hz. The constant dc field was either $\mu_0 H = (0 \pm 0.03)$ mT or (0.6 ± 0.1) mT.

3. RESULTS AND DISCUSSION

Figure 1 shows the real χ' and the imaginary parts χ'' of the ac susceptibility *vs* temperature T for the samples $t = 0.9$ nm (a) and 1.0 nm (b) under four different conditions. Curves 1 and 1′ are measured at the ac frequency $f = 0.1$ and Curves 2 and 2′ at 1 Hz, whereas for Curves 1 and 2 an ac field amplitude of $\mu_0 H_{ac} = 0.05$ mT and a dc field of $\mu_0 H = 0$ mT were applied. For Curves 1′ and 2′ an ac field amplitude of $\mu_0 H_{ac} = 0.4$ mT and a dc field of $\mu_0 H = 0.6$ mT were used (see Fig. 2 for an illustration). For both samples a similar behavior is encountered. Both the increase of the

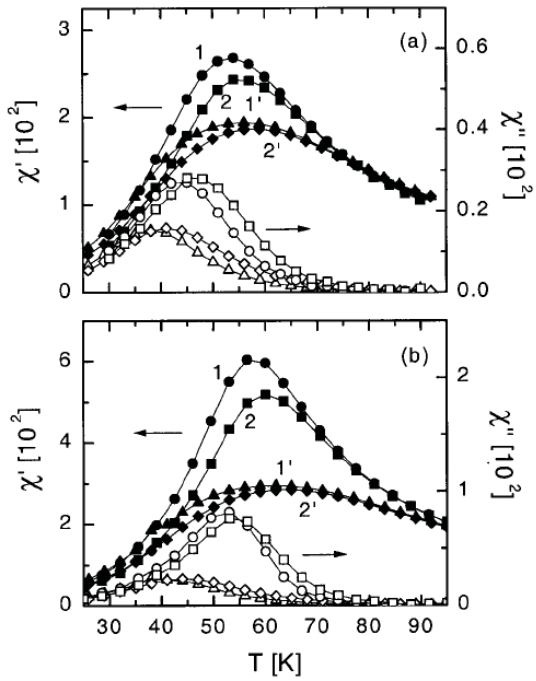

FIGURE 1 χ' and χ'' *vs* T for $t = 0.9$ nm (a) and 1.0 nm (b) measured at constant frequency $f = 0.1$ (Curves 1 and 1′) and 1 Hz (Curves 2 and 2′) with ac field amplitude $\mu_0 H_{ac} = 0.05$ mT and dc field $\mu_0 H = 0$ mT (Curves 1 and 2) and ac field amplitude $\mu_0 H_{ac} = 0.4$ mT and dc field $\mu_0 H = 0.6$ mT (Curves 1′ and 2′), respectively.

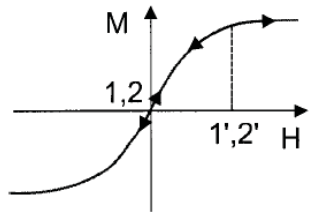

FIGURE 2 Schematic drawing of the measurement conditions relevant for the data as numbered in Fig. 1 (see text). The solid curve shows $M(H)$ without hysteresis.

probing ac field amplitude and the application of a bias field result in a suppression of the amplitude of the real part $\chi'(T)$ and a shift ΔT_m of the peak to higher temperatures. Quantitatively the shift is $\Delta T_m(1'–1)$ =2.2 (3.8) K and $\Delta T_m(2'–2)$ = 2.3 (3.6) K for t = 0.9 (1.0) nm, respectively. The imaginary part $\chi''(T)$ is also suppressed, but the inflection point at T_f is shifted to lower temperatures, ΔT_f (1′–1) = 6.0 (–10.1) K and ΔT_f (2′–2) = –6.2 (–8.2) K for t = 0.9 (1.0) nm, respectively. This behavior is well known from other SG systems and model calculations (Canella and Mydosh, 1972; Barbara *et al.*, 1981) and can be explained in terms of a competition between the noncritical linear susceptibility and the critical nonlinear susceptibility. In other words, the suppression of both the real and the imaginary parts reflects the obvious fact that the $M(H)$ curve becomes increasingly nonlinear when increasing the ac amplitude and/or the bias field (see Fig. 2).

Next we studied the frequency spectra, $\chi'(f)$ and $\chi''(f)$. Figures 3 and 4 (t = 0.9 and 1.0 nm respectively) show the real χ' (a) and the imaginary part χ'' (b) as functions of the ac frequency f for different temperatures T = 45, 50, 55 and 60 K in zero-field and $\mu_0 H_{ac}$ = 0.05 mT. While some negative curvature still indicates a well-defined dispersion step at $f > 10^3$ Hz for T > 60K, this step becomes gradually broadened as T decreases. At low T the real parts show nearly constant negative slopes, thus corresponding to an extremely broad dispersion step. The imaginary parts reveal extremely broad peaks, which strongly shift to lower frequencies with decreasing temperature. Obviously our SSG system exhibits a very wide distribution of relaxation times with a pronounced temperature dependence.

A satisfactory description of the data is provided by the phenomenological Cole–Cole model (Cole and Cole, 1941; Jonscher, 1983) and was successfully applied e.g., to 2D (Dekker *et al.*, 1989; Hagiwara, 1998) or pseudo-1D SG systems (Ravindran *et al.*, 1989). The complex ac susceptibility, $\chi = \chi' - i\chi''$, is written in the Cole–Cole model as (Jonscher, 1983)

$$\chi(\omega) = \chi_S + \frac{\chi_0 - \chi_S}{1 + (i\omega\tau_c)^{1-\alpha}}, \tag{2}$$

where χ_0 and χ_S are the isothermal (low-f) and adiabatic (high-f) susceptibilities, respectively, τ_c is the characteristic relaxation time and α a measure of the polydispersivity of the system. The case α =0 yields the standard Debye-type relaxator with one single relaxation frequency, as found, *e.g.,* in the case of a monodisperse ensemble of noninteracting superparamagnetic particles obeying Eq. (1). The limiting case

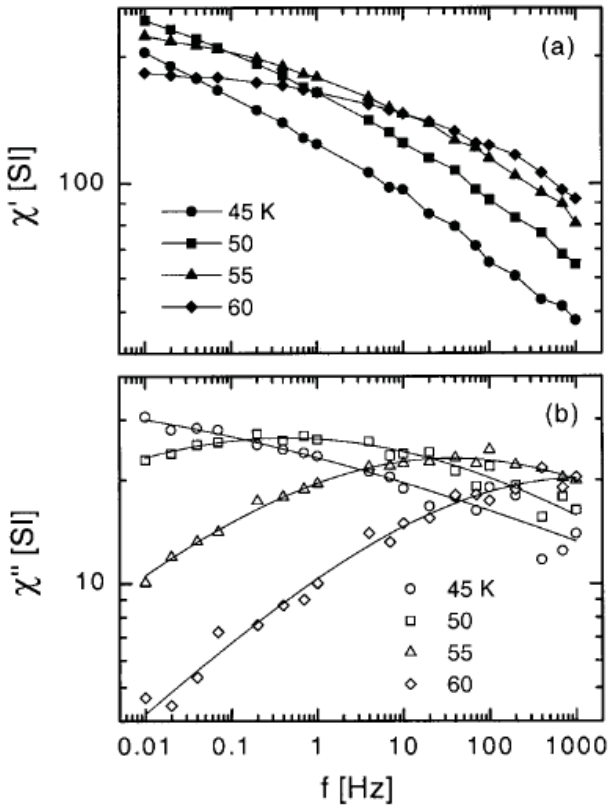

FIGUR E 3 χ' (a) and χ'' (b) *vs f* at different temperatures $T = 45$, 50, 55 and 60 K for the $t =$ 0.9 nm sample in zero-field and $\mu_0 H_{ac} = 0.05$ mT. The lines in (a) are guides to the eyes and in (b) best fits according to Eq. (4).

$\alpha = 1$ corresponds to an infinitely wide distribution of relaxation times. In SG systems one expects values of α near to 1.

After decomposing Eq. (2) into its real and imaginary parts it is possible to perform a fit to the data as shown in Figs. 3 and 4. One finds (compare to Dekker *et al.*, 1989; Ravindran *et al.*, 1989)

$$\chi'(\omega) = \chi_S + \frac{\chi_0 - \chi_S}{2}\left(1 - \frac{\sinh[(1-\alpha)\ln(\omega\tau_c)]}{\cosh[(1-\alpha)\ln(\omega\tau_c)] + \cos[(1/2)(1-\alpha)\pi]}\right) \quad (3)$$

$$\chi''(\omega) = \frac{\chi_0 - \chi_S}{2}\left(\frac{\sin[(1/2)(1-\alpha)\pi]}{\cosh[(1-\alpha)\ln(\omega\tau_c)] + \cos[(1/2)(1-\alpha)\pi]}\right), \quad (4)$$

where $\omega = 2\pi f$. Best results are obtained, when fitting to the imaginary part $\chi''(f)$, since only three parameters, $\chi_0 - \chi_S$, $(1 - \alpha)$ and τ_c are needed in this case.

Figure 5 shows the results from the fitting, τ_c (open circles) and α *vs T* (open diamonds) for both samples, $t = 0.9$ (a) and 1.0 nm (b). One finds that the characteristic relaxation time τ_c is increasing with decreasing temperature. It changes by eight (a) or ten orders (b) of magnitude, respectively. By this kind of extraction of τ_c one has

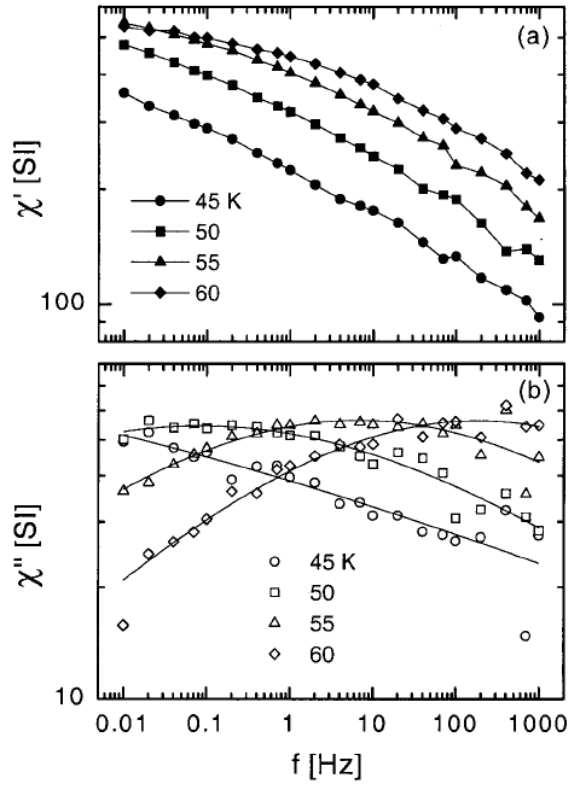

FIGURE 4 χ' (a) and χ'' (b) vs f at different temperatures $T = 45$, 50, 55 and 60 K for the $t = 1.0$ nm sample in zero-field and $\mu_0 H_{ac} = 0.05$ mT. The lines in (a) are guides to the eyes and in (b) best fits according to Eq. (4).

access to an extremely wide timescale and is, hence, more advantageous compared to the standard method of extracting τ_c from the $\chi'(T)$ data. It is straightforward to perform a fit of the $\tau_c(T)$ data to a critical power-law, which was already used in previous publications (Kleemann *et al.*, 2001; Petracic *et al.*, 2002), $\tau_c = \tau_0(T/T_g - 1)^{-zv}$ (solid line). It yields reasonable results, but the value of zv must be kept restricted or even fixed to $zv = 9$. Then we obtain $\tau_0 = (5.0 \times 10^{-8} \pm 5.1 \times 10^{-8})$s, $T_g = (42.63 \pm 0.18)$K and $zv = 9.0 \pm 0.7$ ($t = 0.9$ nm) and $\tau_0 =_{\delta} 3.46 \times 10^{-8} \pm 2.1 \times 10^{-10})$s, $T_g = (43.9354 \pm 0{:}0002)$K and $zv = 9$ fixed ($t = 1.0$ nm), respectively. In the case of $t = 0.9$ nm the values for T_g and τ_0 correspond well to the values obtained previously (Kleemann *et al.*, 2001; Petracic *et al.*, 2002). This does not apply to the $t = 1.0$ nm sample, where $T_g \approx 44$ K differs strongly from the value shown above, $T_g \approx 49$ K. Interestingly the Cole–Cole fit to the $T = 45$ K data for $t = 1.0$ nm does not converge (encircled data points in Fig. 5(b)) leading to the conclusion that the data emerge from the nonergodic regime, $T < T_g$. It is worth to mention that the fit to the modified power law according to Souletie and Tholence (1985), $\tau_c = \tau_0(1 - T_g/T)^{-zv}$ (broken line), yields similar values, *i.e.* $\tau_0 = (2{:}67 \times 10^{-9} \pm 2.9 \times 10^{-9})$s, $T_g = (43.19 \pm 0.11)$ K and $zv = 9.0$ fixed ($t = 0.9$ nm) and $\tau_0 = (3.4 \times 10^{-10} \pm 6.2 \times 10^{-10})$s, $T_g = (44.004 \pm$

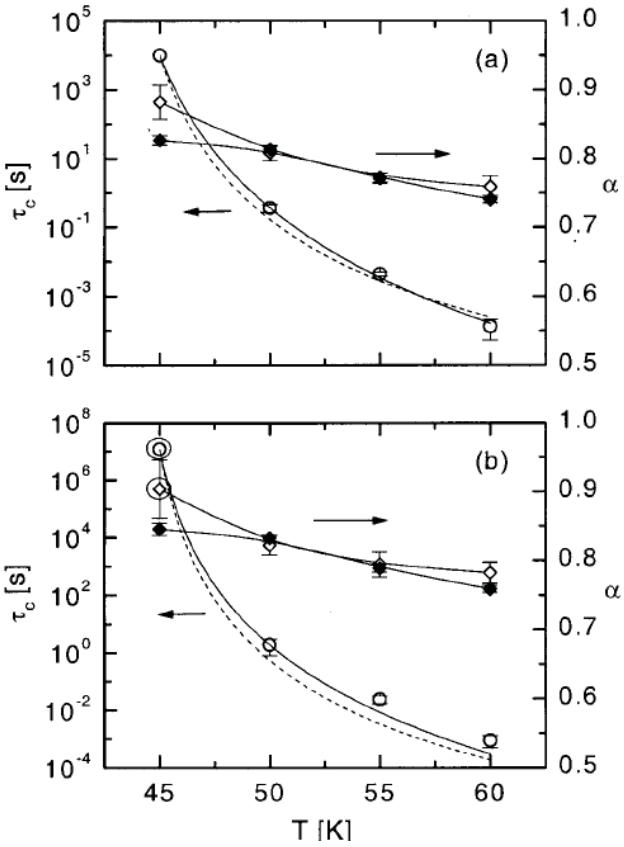

FIGURE 5 Results from Cole–Cole fits to the data shown in Figs. 3, 4 and 6, for $t = 0.9$ (a) and 1.0 nm (b). The characteristic relaxation times τ_c (open circles) are best fitted to a critical power law (solid and broken lines; see text). The polydispersivity exponent α *vs T* as obtained from fits to Eq. (4) (open diamonds) and to Eq. (5) (solid diamonds), respectively, are connected by eye-guiding lines. Encircled data points are results from nonconverging fits.

0036) K and $zv = 10$ fixed ($t = 1.0$ nm), respectively. It is not possible to judge about the advantage of this method here.

The exponent α increases, as expected, with decreasing temperature (Fig. 5). Its high value ($\alpha \approx 0.8$) meets the expectation, that a SG system should have a very broad distribution of relaxation times (Mydosh, 1993).

Often susceptibility data are presented in a way, where the imaginary part is plotted against the real part (Cole–Cole plot), $\chi''(\chi')$ (Cole and Cole, 1941; Jonscher, 1983), where a classic Debye-relaxator should yield a perfect semicircle, centered on the χ'-axis at $(\chi_0 + \chi_S)/2$ and with radius $(\chi_0 - \chi_S)/2$. The apex of the semicircle corresponds to $\omega\tau_c = 1$. Nonzero α has the effect to depress the semicircle such that the angles between the χ'-axis and the tangents at $\omega = 0$ and $\omega \to \infty$ are $\mp (1 - \alpha)\pi/2$, respectively. Figure 6 shows the susceptibility data for $t = 0.9$ (a) and 1.0 nm at different temperatures $T = 45$, 50, 55 and 60 K. The above derived expressions for the

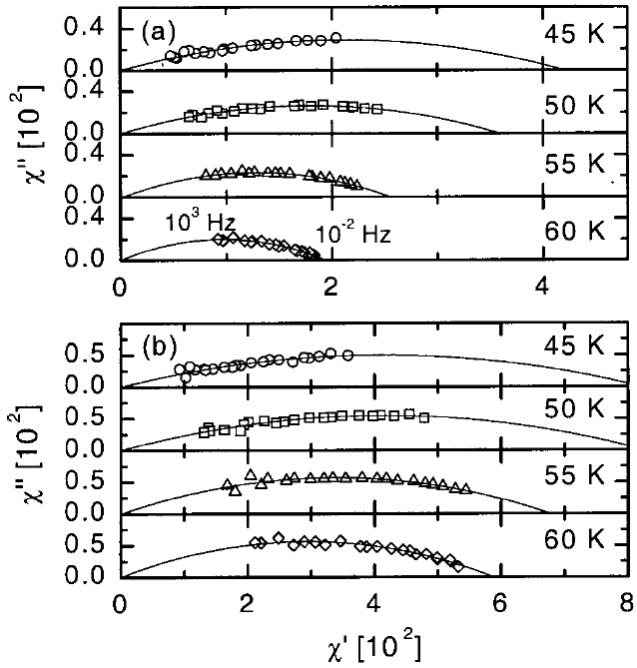

FIGURE 6 Cole-Cole plots of χ'' *vs* χ' for $t = 0.9$ (a) and 1.0 nm (b) at different temperatures and frequencies as indicated. The solid lines are best fits according to Eq. (5).

real and imaginary parts (Eqs. (3) and (4)) can be expressed in the form (Hagiwara, 1998)

$$\chi''(\chi') = -\frac{\chi_0 - \chi_S}{2\tan[(1-\alpha)\pi/2]} + \left\{(\chi' - \chi_S)(\chi_0 - \chi') + \frac{(\chi_0 - \chi_S)^2}{4\tan^2[(1-\alpha)\pi/2]}\right\}^{1/2}. \quad (5)$$

The fit yields similar results for $\alpha(T)$ compared to those from the fit to the imaginary part $\chi''(f)$ (Fig. 5, solid *vs* open diamonds). It should be noticed that $\chi_S = 0$ in all cases, *i.e.* no measurable response is expected at frequencies above single particle flip frequencies. This corroborates the model of ferromagnetic order within each superparamagnetic particle.

4. CONCLUSION

The dynamical susceptibility of the SSG system $[Co_{80}Fe20(t)/Al_2O_3\ (3\ nm)]_{10}$ ($t = 0.9$ and 1.0 nm) was studied under the influence of a bias field and in view of its polydispersivity within the framework of a Cole–Cole description. Cole–Cole fits yield reasonable values for the characteristic relaxation time τ_c of the system and for its polydispersivity exponent α. The relaxation time can be well described by a critical power-law dependence. One should note that by this kind of extraction of τ_c one has access to an extremely wide timescale of eight or ten orders of magnitude. Reasonably large values, $\alpha \approx 0.8$,

are obtained, which are typical of SG systems. The Cole–Cole plots of the susceptibility data confirm the SG characteristic, i.e. one observes a strongly flattened semicircle.

Acknowledgment

The authors acknowledge financial support by the German Science Council through the Graduate College "Structure and Dynamics of Heterogeneous Systems."

References

Barbara, B., Malozemoff, A.P. and Imry, Y. (1981). Field-dependence of the dc susceptibility of spin glasses. *Physica B & C,* **108**, 1289.

Brown, W.F. (1963). Thermal fluctuations of a single-domain particle. *Phys. Rev.,* **130**, 1677.

Canella, V. and Mydosh, J.A. (1972). Magnetic ordering in gold-iron alloys. *Phys. Rev. B,* **6**, 4220.

Chen, X., Sichelschmidt, O., Kleemann, W., Petracic, O. *et al.* (2002). Domain wall relaxation, creep, sliding and switching in superferromagnetic discontinuous $Co_{80}Fe_{20}$-Al_2O_3 multilayers. *Phys. Rev. Lett.,* **89**, 137203.

Cole, K.S. and Cole, R.H. (1941). Dispersion and absorption in dielectrics. *J. Chem. Phys.,* **9**, 341.

Dekker, C., Arts, A.F.M., de Wijn, H.W. and van Duyneveldt, A.J. (1989). Activated dynamics in a two-dimensional Ising spin glass: $Rb_2Cu_{1-x}Co_xF_4$. *Phys. Rev. B,* **40**, 11243.

Djurberg, C., Svedlindh, P., Nordblad, P., Hansen, M.F. *et al.* (1997). Dynamics of an interacting particle system: evidence of critical slowing down. *Phys. Rev. Lett.,* **79**, 5154.

Dormann, J.L., Fiorani, D., Cherkaoui, R., Tronc, E.J. *et al.* (1999). From pure superparamagnetism to glass collective state in γ-Fe_2O_3 nanoparticle assemblies. *J. Magn. Magn. Mater.,* **203**, 23.

Dormann, J.L., Fiorani, D. and Tronc, E.J. (1997). Magnetic relaxation in fine-particle systems. *Adv. Chem. Phys.,* **98**, 283.

Hagiwara, M. (1998). Cole-Cole plot analysis of the spin-glass system NiC_2O_4•$2(2MIz)_{0.49}(H_2O)_{0.51}$. *J. Magn. Magn. Mater.,* **177–181**, 89.

Jonscher, A.K. (1983). *Dielectric Relaxation in Solids.* Chelsea Dielectrics Press, London.

Kakazei, G.N., Pogorelov, Y.G., Lopes, A.M.L., Sousa, J.B. *et al.* (2001). Tunnel magnetoresistance and magnetic ordering in ion-beam sputtered $Co_{80}Fe_{20}/Al_2O_3$ discontinuous multilayers. *J. Appl. Phys.,* **90**, 4044.

Kleemann, W., Petracic, O., Binek, Ch., Kakazei, G.N. *et al.* (2001). Interacting ferromagnetic nanoparticles in discontinuous $Co_{80}Fe_{20}/A1_2O_3$ multilayers: from superspin glass to reentrant superferromagnetism. *Phys. Rev. B,* **63**, 134423.

Mamiya, H., Nakatani, I. and Furubayashi, T. (1999). Slow dynamics for spin-glass-like phase of a ferromagnetic fine particle system. *Phys. Rev. Lett.,* **82**, 4332.

Mydosh, J.A. (1993). *Spin Glasses: An Experimental Introduction.* Taylor & Francis, London.

Néel, L. (1949). Théorie du trainage magnétique des ferromagnétiques en grains fins aver applications aux terres cuites. *Ann. Geophys.,* **5**, 99.

Petracic, O., Kleemann, W., Binek, Ch., Kakazei, G.N. *et al.* (2002). Superspin glass behavior of interacting ferromagnetic nanoparticles in discontinuous magnetic multilayers. *Phase Transitions,* **75**, 73.

Ravindran, K., Rubenacker, G.V., Haines, D.N. and Drumheller, J.E. (1989). Spin-cluster relaxation times in the spin-glass $[(CH_3)_3NH]$ $Co_{0.4}$ $Ni_{0.6}Cl_3$ • $2H_2O$. *Phys. Rev. B,* **40**, 9431.

Sahoo, S., Petracic, O., Binek, Ch., Kleemann, W. *et al.* (2002a). Superspin-glass nature of discontinuous $Co_{80}Fe_{20}/A1_2O_3$ multilayers. *Phys. Rev. B,* **65**, 134406.

Sahoo, S., Sichelschmidt, O., Petracic, O., Binek, Ch. *et al.* (2002b). Magnetic states of discontinuous $Co_{80}Fe_{20}/A1_2O_3$ multilayers. *J. Magn. Magn. Mater.,* **240**, 433.

Sankar, S., Dender, D., Borchers, J.A., Smith, D.J. *et al.* (2000). Magnetic correlations in non-percolated $CoSiO_2$ granular films. *J. Magn. Magn. Mater.,* **221**,1.

Souletie, J. and Tholence, J.L. (1985). Critical slowing down in spin glasses and other glasses: Fulcher versus power law. *Phys. Rev. B,* **32**, 516.

Sousa, J.B., Kakazei, G.N., Pogorelov, Y.G., Santos, J.A.M. *et al.* (2001). Magnetic states of granular layered CoFe-$A1_2O_3$ system. *IEEE Trans. Mag.,* **37**, 2200.

Stappert, S., Dumpich, G., Sahoo, S., Petracic, O. *et al.* (2002*). Transmission Electron Microscopy Studies on Ion-beam Sputtered $Co_{80}Fe_{20}/Al_2O_3$ Discontinuous Bilayers*. Unpublished.

Young, A. (Ed.) (1997). *Spin Glasses and Random Fields,* Series on Directions in Condensed Matter Physics. World Scientific, Singapore.